USF1 defect drives p53 degradation during *Helicobacter pylori* infection and accelerates gastric carcinogenesis

Lionel Costa, Sébastien Corre, Valérie Michel, Krysten Le Luel, Julien Fernandes, Jason Ziveri, Grégory Jouvion, Anne Danckaert, Nicolas Mouchet, David Da Silva Barreira, Javier Torres, Margarita Camorlinga-Ponce, Mario Milco D'Elios, Laurence Fiette, Hilde De Reuse, Marie-Dominique Galibert and Eliette Touati.

Supplementary Information

Results

Cytoplasmic aggregation of USF1 is associated with depletion of p53 and gastric intraepithelial neoplasia in INS-GAS mice infected with Hp

To investigate the clinical relevance of *Hp*-induced cytoplasmic accumulation of USF1, we took advantage of the INS-GAS mouse model in which *Hp* accelerates the development of gastric intraepithelial neoplasia[1,2]. As expected, at 6 and 12 months pi mice developed earlier than non-infected, severe gastric hyperplasia, dysplasia and low-grade gastric intraepithelial neoplasia (figure S6A). IF analysis on gastric tissue sections showed a marked cytoplasmic accumulation of USF1 in *Hp*-infected mice (figure S6B), associated to the decrease of p53 levels, as reported at 12 months pi (figure S6C). These results are consistent with *in vitro* data and confirm that USF1 accumulates overtime pi outside the nuclei of *Hp*-infected gastric epithelial cells, concomitantly to p53 depletion.

Material and methods

Bacteria, cell culture and infection

Human gastric epithelial cells, AGS: gastric adenocarcinoma (CRL-1739, ATCC-LGC) and MKN45 used in this study were cultured in RPMI 1640 medium with 10% fetal bovine serum (FBS) and 1% penicillin-streptomycin. *Hp* strains 7.13[3] and SS1[4] were grown at 37°C on 10% blood agar plates under microaerophilic conditions. Bacterial lysates were obtained by passage through a French press and their proteins concentration determined by Dc Protein assay (Bio-Rad, Hercules, CA, USA).

Cells preparation, immunostaining and microscopy

Cells were fixed on slides with 4% paraformaldehyde (PFA) in 0.1M Phosphate buffer (15735-60S, Electron Microscopy Sciences) for 15min at room temperature (RT), incubated 1h at RT in quenching buffer (NH_4Cl 50mM, PBS). The primary antibodies used were, anti-USF1 (Ab167693, Abcam; 1/100), anti-p53 (FL-393) (sc-6243, Santa Cruz Biotechnology, CA, USA; 1/200) and anti-γH2AX (p-Ser139) (NB100-384, Novus Biologicals 1/2500). The nuclear DNA was stained with NucBlue® Live ReadyProbes® Reagent ((R37605), Thermo Fisher Scientific, USA) and actin stained with Alexa Fluor® 647 Phalloidin (A22287, Thermo Fisher Scientific, USA, 1/100). Sample images were acquired with an Inverted Widefield Microscope Axio Observer Z1 equipped with Apotome grid (Carl Zeiss, Germany) with a Plan-Apochromat 63x1.40 Oil M27 objective. In the case of MMS and H_2O_2 experiments (Figures S8 to S10), image acquisition was performed using a spinning disk SP8 microscope. Random field images were acquired as 211.30 × 211.30 μm^2 with a depth of 100µm at 7µm increment.

Image processing and immunofluorescence quantification

After acquisition, a maximum of intensity projection processing from images were done using automated free plugins of the imageJ v1.50 software interface[5]. Image analysis was carried out using Acapella software (version 2.7, PerkinElmer Life Sciences). The script was subdivided into three object subroutines segmenting successively the nucleus, the cytoplasm, and USF1 spots within the cytoplasm and membrane surrounding area of each cell. First the cell regions are determined by nuclei and cytoplasm detection library modules using the appropriated channel images. Spots corresponding to USF1 foci are detected in the cytoplasm body areas using Alexa Fluor AF488 channel. The parameters of the detected spots, (e.g. number, intensity) are added to the cell object list. A number of numerical output values is generated. Spot candidates are detected as local intensity maximums within cytoplasm. Thereupon the

spots are selected by contrast and intensity parameters. For each condition, 5 microscopic fields were analysed and n=150 to 220 cells quantified.

Analysis of gene expression

Human gastric epithelial cells MKN45 were infected with the *Hp* strains at a multiplicity of infection (MOI) of 100 bacteria per cell for 2 and 24h.

Total RNA was isolated from MKN45 cells, from mice stomach or from human gastric biopsies using the RNeasy Mini Kit (Qiagen). It was reverse-transcribed using Superscript® III Reverse transcriptase (Invitrogen) and amplified with Power Sybr Green PCR Master Mix (Applied Biosystems) using the StepOne^{TM} Plus Real-Time PCR system (Applied Biosystems). Primers used for each gene are listed in the table S2. Target genes were normalized according to the *18SrRNA* genes for analysis in MKN45 cells. The analysis of *USF1* gene expression in human gastric biopsies was performed using the Real-Time PCR TaqMan gene expression kit (Applied Biosystems), normalized according to the *18SrRNA* gene, with commercial primers reported in the supplementary table S1. Amplification PCR consisted in 40 cycles of 15 seconds at 95°C and 1 min 60°C. Data were analysed by StepOne Plus RT-PCR software v2.1. Experiments were performed in triplicate.

Table S1: List of human primers used for the quantification of gene expression

Gene name	Primer
FH1_USF1	TCACAAAGAATTGACCAGTG
RH1_USF1	GACGCACTATACTTACTTCC
FH1_TP53	ACCTATGGAAACTACTTCCTG
RH1_TP53	ACCATTGTTCAATATCGTCC
hCSA-F	GTTCCAATGGAGAAAACACACTT
hCSA-R	CCATATGGTACAAAAACAAATTCTGA
hHR23A-F	GTCACCATCACGCTCAAAAC
hHR23A-R	CTATCTTCTCCTTTAGCACCTTCAC
hGADD45a-F	TCAGCGCACGATCACTGTC
GADD45a-R	CCAGCAGGCACAACACCAC
hp21/CDKN1A-F	CTGGAGACTCTCAGGGTCGAA
hp21/CDKN1A-R	CGGCGTTTGGAGTGGTAGA
FH1_RN18S1	ATCGGGGATTGCAATTATTC
RH1_RN18S1	CTCACTAAACCATCCAATCG
FH1_TBP	GCCAAGAGTGAAGAACAG
RH1_TBP	GAAGTCCAAGAACTTAGCTG

Primers for TaqMan® Gene Expression Assays
(Applied Biosystems, Foster City, CA)

Gene name	Primer
Human USF1	Hs00982868_m1
Human 18S	Hs99999901_s1

Analysis of protein levels by Western blot

After co-culture with *Hp*, cells were lysed in NP-40 buffer containing protease inhibitors; 30 µg per lane was separated on a 12 % Mini-PROTEAN® TGX Stain-Free™ Precast Gels (BioRad) and transferred onto Trans-Blot® Turbo™ Midi PVDF Transfer Packs using a Trans-Blot® Turbo™ Transfer System (BioRad). USF1 (EPR6430 ab125020 ; Abcam, dilution 1/5000), USF2 antibodies ((C-20) Ref sc-862 ; Santa Cruz Biotechnology, CA,USA; dilution 1/200), GAPDH ((FL-335) sc-05778, Santa Cruz Biotechnology, CA,USA; 1/100), p53 ((FL-393) sc-6243, Santa Cruz Biotechnology, CA,USA; dilution 1/100)**,** β-Actin ((BA3R) (MA5-15739), ThermoFisher Scientific, USA, dilution 1/5000) were used followed by a goat anti-rabbit IgG-HRP (sc-2054, Santa Cruz Biotechnology, CA,USA; 1/10000) or Anti-Mouse IgG

HRP Conjugate ((W402B), Promega, Dilution 1/5000). Detection was performed using the SuperSignal™ West Femto Maximum Sensitivity Substrate (ThermoFisher Scientific, USA) and a ChemiDoc XRS (Bio-Rad). Western blot data were quantified by densitometry using Image Lab software (Bio-Rad).

Analysis of protein complexes by proximity ligation assay (PLA)

MKN45 Cells, grown on glass coverslips, were fixed with 4% PFA in 0.1M Phosphate buffer (15735-60S, Electron Microscopy Sciences) for 15min at RT and PLA was performed using the kits ((DUO92007) Duolink® in Situ Detection Reagent Orange, (DUO92001) Duolink® in Situ PLA® Probe Anti-Mouse PLUS, (DUO92005) Duolink® in Situ PLA® Probe Anti-Rabbit MINUS, Sigma) according to the manufacturer's protocol. After blocking, the reaction with primary antibodies, rabbit anti-USF1 (C20, sc-229, Santa Cruz Biotechnology, CA, USA, 1/100) and mouse anti-p53 (1C12, #2524, Cell Signaling Technologies, MA, USA, 1/100) was performed. Protein-protein interactions are revealed with species-specific secondary antibodies conjugated to complementary oligonucleotide allowing ligation and amplification of complementary DNA if the two proteins are in close proximity[6].

In silico analyses

Heatmaps were generated with R-packages heatmap3[7]. Gene Set Enrichment Analysis were performed using GSEA 3.0 tool from the Broad Institute software (http://software.broadinstitute.org/cancer/software/gsea)[8]. STAD TCGA expression data were obtained using cBioPortal (https://www.cbioportal.org/)[9].

Expression data were obtained from GSE2685[10], GSE55699[11], .E-GEOD-74577 (Hong et al) (https://www.ebi.ac.uk/arrayexpress/experiments/), GSE5081[12] and E-MEXP-1135[13] (https://www.ebi.ac.uk/arrayexpress/experiments/E-MEXP-1135/).

Gene set enrichment analysis (GSEA version 3.0)[9] was performed by ranking TCGA (STAD, low survival versus high survival for gastric cancer patients) genes based on their cZ-score as metric. Different ranked lists were used including low (top 25%) versus high (top 25%) survival for gastric cancer patients (STAD, n=188). The following gene signatures were analyzed for enrichment: KEGG pathways gene sets, using p53 target genes (FISCHER_DIRECT_P53_TARGETS_META_ANALYSIS Gene set, n=298) or using USF putative target genes (USF_01 Gene set, n=256) (http://software.broadinstitute.org/gsea/msigdb).

Genotyping of INS-GAS mice

Usf1$^{-/-}$[14] and *Usf1*$^{+/+}$ wild-type (WT) mice (C57BL/6j 129SV) previously provided by S. Vaulont (Institut Cochin, Paris, France) were maintained under specific pathogen free (SPF) conditions and reproduced in the animal facility (University of Rennes) (ARCHE-BIOSIT UMS 34380 (N°A35 23840). The USF1 deletion in *Usf1*$^{-/-}$ mice was validated by PCR using the following primers: USF1-Int2-F (WT or KO): TTGGGAACCATGTTACGAGG, USF1-IRES-R (KO): TACCCGGGGATCCTCTAGAG, and USF1-Int4-R (WT): ACAGCTACTCCTCCAAGCCAC.

INS-GAS mice[1,2] (FVB/N genetic background) were breeded at the animal facility (Institut Pasteur, Paris), from couples provided by TC Wang (Columbia University College, NY, USA). The INS-GAS trans-gene[2] was confirmed in all mice by tail genotyping using the PCR primers: Forward: 5' TGATCTTTGCACTGGCTCTG3' and Reverse: 5'TCCATCCATCCATAGGCTTC3'.

Hp infection of mice

For both mouse models, 14 5-6 weeks-old male mice were orally inoculated with *Hp* SS1 (10^8

colony-forming units (cfu)/100µl) at days 1 and 3; non-infected mice (n=14) received peptone broth. After 6 (9 months for *Usf1*$^{-/-}$) and 12 months mice were sacrificed (n=7/group). Gastric tissues were collected for histopathological and immunofluorescence analysis as already reported[15]. *Hp* gastric colonization was evaluated as previously described[16].

Histopathology analysis of gastric lesions

Stomach samples from non-infected and infected mice were fixed in RCL2® (Alphelys, France) and embedded in low-melting-point paraffin wax (Poly Ethylene Glycol Distearate; Sigma, USA). 4 µm-thick sections were stained by hematoxylin and eosin treatment (H&E) and examined blindly for histopathologic lesions. Histologic alterations (i.e. inflammation, ulceration, foveolar hyperplasia, intestinal metaplasia, parietal cell loss, dysplastic changes of the gastric mucosa and herniation), which were semi-quantitatively evaluated based on a scoring system with five severity grades (1: minimal, 2: mild, 3: moderate, 4: marked and 5: severe) were characterized as previously described[15].

Immunofluorescence on gastric tissues from mice

Gastric tissue sections (4 µm) were taken from infected and control mice were dewaxed (5min (2x) Xylene, 2min (2x) Ethanol 100%), rehydrated 5min in PBS-1X, blocked 1h in PBS-1X + 3% BSA + 0.4% Triton X-100 at room temperature (RT). Then incubated with the primary antibody anti-USF1 ((C-20) sc-229, Santa Cruz Biotechnology, CA, USA; dilution 1/100), anti-p53 monoclonal Antibody (SP5) MA5-14516, ThermoFisher Scientific, USA; dilution 1/100) in PBS-1X, 0.4% Triton X-100 and 3% BSA overnight at 4°C. A secondary Goat anti-rabbit IgG (H+L) Highly Cross-Adsorbed Secondary Antibody, Alexa Fluor 546 ((A11035), ThermoFisher Scientific, USA, dilution 1/400) in PBS-1X + 0,4% Triton X-100 + 3% BSA was applied. The nuclear DNA was stained with NucBlue® Live ReadyProbes® Reagent

((R37605), ThermoFisher Scientific, USA). USF1 staining were observed with an Inverted widefield Microscope Axio Observer ZI equipped with Apotome grid (Carl Zeiss, Germany) using a 63x/1.4 oil immersion objective. p53 staining were acquired at 20X with Axio scan Z1 Zeiss® by using Zen software.

References

1. Fox J, Rogers A, Ihrig M, *et al. Helicobacter pylori* associated gastric cancer in INS-GAS mice is gender specific. *Can Res* 2003;63:942-50.
2. Wang T, Dangler C, Chen D, et al. Synergistic interaction between hypergastrinemia and Helicobacter infection in a mouse model of gastric cancer. *Gastroenterology* 2000;118:36-47.
3. Franco AT, Israel DA, Washington MK, *et al.* Activation of beta-catenin by carcinogenic *Helicobacter pylori. Proc Natl Acad Sci U S A* 2005;102:10646-51.
4. Lee A, O'Rourke J, Ungria M, *et al.* A standardized mouse model of *Helicobacter pylori* infection : introducing the Sydney strain. *Gastroenterology* 1997;112:1386-1397.
5. Schindelin J, Arganda-Carreras I, Frise E, *et al.* Fiji: an open-source platform for biological-image analysis. *Nat Methods* 2012;9:676-82.
6. Soderberg O, Gullberg M, Jarvius M, *et al.* Direct observation of individual endogenous protein complexes in situ by proximity ligation. *Nat Methods* 2006;3:995-1000.
7. Zhao S, Guo Y, Sheng Q, *et al.* Advanced heat map and clustering analysis using heatmap3. *Biomed Res Int* 2014;2014:986048.
8. Subramanian A, Tamayo P, Mootha VK, *et al.* Gene set enrichment analysis: a knowledge-based approach for interpreting genome-wide expression profiles. *Proc Natl Acad Sci USA* 2005;102:15545-50.
9. Gao J, Aksoy BA, Dogrusoz U, *et al.* Integrative analysis of complex cancer genomics and clinical profiles using the cBioPortal. *Sci Signal* 2013;6:l1.
10. Hippo Y, Taniguchi H, Tsutsumi S, *et al.* Global gene expression analysis of gastric cancer by oligonucleotide microarrays. *Cancer Res* 2002;62:233-40.
11. Koeppel M, Garcia-Alcalde F, Glowinski F, *et al. Helicobacter pylori* Infection Causes Characteristic DNA Damage Patterns in Human Cells. *Cell Rep* 2015;11:1703-1713.

12. Galamb O, Gyorffy B, Sipos F, *et al. Helicobacter pylori* and antrum erosion-specific gene expression patterns: the discriminative role of CXCL13 and VCAM1 transcripts. *Helicobacter* 2008;13:112-26.
13. Vivas JR, Regnault B, Michel V, *et al.* Interferon gamma-signature transcript profiling and IL-23 upregulation in response to *Helicobacter pylori* infection. *Int J Immunopathol Pharmacol* 2008;21:515-26.
14. Vallet VS, Casado M, Henrion AA, et al. Differential roles of upstream stimulatory factors 1 and 2 in the transcriptional response of liver genes to glucose. *J Biol Chem* 1998;273:20175-9.
15. Touati E, Michel V, Thiberge J, *et al.* Chronic *Helicobacter pylori* infections induce gastric mutations in mice. *Gastroenterology* 2003;124:1408-1419.
16. Ferrero RL, Thiberge JM, Huerre M, *et al.* Immune responses of specific-pathogen-free mice to chronic *Helicobacter pylori* (strain SS1) infection. *Infect Immun* 1998;66:1349-55.
17. Bussière FI, Michel V, Memet S, *et al. H. pylori*-induced promoter hypermethylation downregulates USF1 and USF2 transcription factor gene expression. *Cell Microbiol* 2010;12:1124-33

Legend of supplementary figures

Figure S1. Involvement of p53 pathway and USF1 targets in gastric carcinogenesis.

(A) Survival curve for GC patients (TCGA, STAD n=188) according to *SLC7A2* mRNA level, a most discriminant gene (25% top low: blue or 25% to high: red). (B) Survival curve for GC patients according to *USF1* and *TP53* mRNA levels (low: green, medium: blue or high: red). (C) Correlation of *USF1* and *TP53* mRNA level expression from the stomach of gastric adenocarcinoma patients (TCGA, Provisional n=478; cBioPortal: https://www.cbioportal.org/). Each symbol corresponds to one patient. (D) Expression Heatmap, in GC patients associated with both low and high survival, and depicting median mRNA expression of genes specific to the different KEGG pathways (KEGG gene sets), and that have been shown to be enriched after Gene Set Enrichment Analysis (GSEA, broadinstitute), (E-F) Gene Set Enrichment Analysis (GSEA, broadinstitute) in GC patients associated with both low and high survival, (E) using p53 target genes (FISCHER_DIRECT_P53_TARGETS_META_ANALYSIS Gene set, n=298) or (F) using USF putative target genes (USF_01 Gene set, n=256). (G) Relative *USF1* gene expression in gastric biopsies from GC patients (n=34) measured by qRT-PCR (tumoral *vs* adjacent tissue), comparison between *Hp*-positive and *Hp*-negative patients. A trend for a lower *USF1* gene expression in the tumor-tissue *vs* adjacent-tissue is observed in *Hp*-positive patients compared to *Hp*-negative patients. (Mann-Whitney test*; Hp*-positive vs *Hp*-negative).

Figure S2. p53 and USF1 loss correlate with the deregulation of their target genes and low survival of GC patients

Expression Heatmap depicting mRNA expression of top 50 p53-target genes (Fisher_direct_p53_targets_meta_analysis, GSEA) and top 50 putative USF1-target genes (Genes having at least one occurrence of the transcription factor binding site V$USF_01 (v7.4 TRANSFAC) in the regions spanning up to 4 kb around their transcription starting sites,

GSEA), that have been significantly enriched in both low and high survival GC population. p53 and USF1 target genes (p53-targets: orange and pink; USF1-targets: blue and green; common targets: black), previously correlated with low (pink and green) or high survival (orange and blue) using expression data from Hippo and coll[10] comparing noncancerous and cancerous tissues (Figure 1D).

Figure S3. Lack of USF1 leads to inhibition of the expression of p53- and USF1-target genes in *Hp*-infected *Usf1*$^{-/-}$ mice.

(A) Expression Heatmap depicting mRNA expression of p53 and USF1 target genes previously correlated with low or high survival (figure 1A-C), using data from GSE5081 (Galamb and coll)[12] for gastric biopsies of patients with *Hp*-positive and *Hp*-negative antrum erosions (E+) (8/8) and adjacent normal mucosae (E^{-}) (8/8) (p53-targets: orange and pink; USF1-targets: blue and green; common: black). (B) Log-fold enrichment for p53 and USF1 target genes expression in chronically *Hp*SSI infected and non-infected mice after 12 months from E-MEXP-1135 (Vivas and coll)[13] (C) Gastric colonization measured from stomach fragments isolated from *Usf1*$^{+/+}$ and *Usf1*$^{-/-}$ mice sacrificed after 9 and 12 months of infection with *Hp*SS1. The non-infected control groups are not colonized and are not reported. The number of colonies forming unit (cfu) was determined as previously described[16]. (D) Expression of the p53-targets *GADD45, CDKN1A*, *PCNA*; *CSA*, *HR23A* genes related to the NER pathway regulated by both USF1 and p53, and *RAB31* an USF1-target measured by RT-qPCR, on RNA isolated from the stomach of *Usf1*$^{-/-}$ and *Usf1*$^{+/+}$ mice infected for 12 months as described in the supplementary methods. The absence of USF1, in *Usf1*$^{-/-}$ mice, leads to the inhibition of the expression of *HR23A* and *CSB*, as well as *GADD45*, *PCNA* and *RAB31* gene expression in infected mice. Mean±SD. Student t test; infected *vs* non-infected (*p<0.05; **p<0.01; ***p<0.001; ****p<0.0001).

Figure S4. *Hp* total extracts inhibit USF1 and p53 levels and impair host DNA repair function.

Human adenocarcinoma gastric epithelial cells MKN45 cells were treated with total extracts of the strain *Hp*7.13 at 50µg/ml and 100µg/ml for 2h and 24h. Control cells were not treated. (A) *USF1,* (C) *TP53* and (E) *CSA* and *HR23A* mRNA were quantified by RT-qPCR. (B) USF1 (D) p53 and GAPDH (loading control) western blots analysis. Under this condition, an inhibition of *USF1* gene expression was observed, as well as protein level at 24h pi, in agreement with a cag-PAI-independent regulation, as we previously observed[17]. The *TP53* gene expression and protein level are also down-regulated, as *CSA* and *HR23A*. The histogram below corresponds to the immunoblot quantification normalized to GAPDH as described in the methods section. Mean±SD, n=3. Student t test; infected *vs* non-infected (** $p<0.01$; ****$p<0.0001$). (F) Analysis of γH2AX levels indicating the presence of DSB in MKN45 cells infected with *Hp* 7.13 at MOI 100:1 for 2h and 24h, γH2AX immunofluorescence staining (red) and nuclei (Hoechst, blue). Experiments have been done in duplicate with 5 to 7 microscopic fields analysed for each condition. Scale bar: 2µm.

Figure S5. The *Hp* strain SS1 used to colonize the mice stomach also inhibits USF1 and p53 level *in vitro*.

Human adenocarcinoma gastric epithelial cells MKN45 cells were infected with the *Hp* strain SS1 at MOI 100:1 for 2h and 24h. Control cells were not infected. (A) *USF1, (C) TP53* mRNA were quantified by RT-qPCR and (B) USF1, (D) p53 protein levels analyzed by western blot. *Hp*SS1 also inhibits USF1 and p53 gene expression and protein level, but at a lower extent compared to *Hp*7.13 (see figure 3). The histogram below corresponds to the immunoblot quantification normalized to GAPDH as described in material and methods. Mean±SD, n=3. Student t test; infected *vs* non-infected (**$p<0.01$; *** $p<0.001$).

Figure S6. *Hp* leads to USF1 cytoplasmic accumulation in the gastric mucosa of INS-GAS mice and induces gastric cancer lesions.

Mice were orally infected with *Hp* SS1 for 6 and 12 months, and gastric lesions compared to non-infected mice. (A) Representative gastric histological changes in *Hp*-infected mice (b, d) and non-infected (NI) (a, c) after 6 (a, b) and 12 months (c, d) on H&E stained paraffin sections. Scale bar: 500 μm. Infected mice at 6 months pi (b) show hyperplastic and metaplastic lesions compared to controls (a). At 12 months, infected-mice (d) display more severe hyperplasia and dysplasia than uninfected-mice (c) with low-grade gastric intraepithelial neoplasia, as defined by dysplasia and herniation into the sub-mucosa. (B) USF1 IF (green) and nuclei (Hoechst, blue) in gastric tissue sections after 6 (left part) and 12 months (right part), showing a predominant USF1 staining and accumulation in the cytoplasm of gastric cells, observed concomitantly with the presence of gastric intraepithelial neoplasia. Scale bar, 20μm. (C) p53 immunostaining (green) in gastric tissue section from *Hp*-infected and non-infected INS-GAS mice after 12 months. Also in this genetic background and concomitantly to the development of gastric intraepithelial neoplasia, *Hp* inhibits p53 levels, in parallel to USF1 delocalisation.

Figure S7. Induction of DSB in CPT-treated cells infected with *Hp*.

IF analysis of γH2AX levels indicating the presence of DSB in MKN45 cells treated with CPT (50nM) and infected or not with *Hp*7.13 at MOI 100:1 for 24h. γH2AX (red) and nuclei (Hoechst, blue). Experiments have been done in duplicate with 5 to 7 microscopic fields analysed for each condition.

Figure S8. The induction of USF1 foci is *Hp*-dependent and not observed in MMS-treated cells

(A) IF analysis of USF1 and p53 levels and localization, in MKN45 cells treated or not with MMS (1mM) and infected with *Hp* 7.13 or not-infected, for 2 and 24h. p53 (red), USF1 (green), nuclei (Hoechst, blue) and phalloidin actin staining (grey). The delocalization and accumulation of USF1 are specifically observed in the cytoplasm and membrane surrounding area of *Hp*-infected/MMS-treated cells. Scale bar 5µm. (B) Quantification of USF1 and p53 cellular IF intensity. IF intensity measured for USF1 and p53 is decreased in MMS-treated cells and *Hp* infected (n=150-220 cells/condition). (C) Quantification of USF1 spots number/cell as in figure 5, showing that USF1 foci are only observed in the presence of *Hp* as in the case of CPT±*Hp* cells (see figure 5). (n=150-220 cells/condition), Mann-Whitney test, treated/infected *vs* control ((*p<0.05; ****p<0.0001). Experiments in triplicate with 5-7 fields analysed.

Figure S9. The induction of USF1 foci is *Hp*-dependent and not observed in H_2O_2-treated cells

(A) IF analysis of USF1 and p53 levels and localization, in MKN45 cells treated or not with H_2O_2 (1mM) and infected with *Hp* 7.13 for 2 and 24h. p53 (red), USF1 (green), nuclei (Hoechst, blue) and phalloidin actin staining (grey). The delocalization and accumulation of USF1 are specifically observed in the cytoplasm and membrane surrounding area of *Hp*-infected/H_2O_2-treated cells. Scale bar 5µm. (B) Quantification of USF1 and p53 cellular IF intensity which is decreased in H_2O_2-treated cells and *Hp* infected, as previously observed in CPT (or MMS)-treated/infected cells (n=150-220 cells/condition). (C) Quantification of USF1 spots number/cell as in figure 3. A significant increase of USF1 foci is only observed in the presence of *Hp*. (n=150-220 cells/condition), Mann-Whitney test, treated/infected *vs* control (****p<0.0001). Experiments in triplicate with 5-7 fields analysed.

Figure S10. The formation of USF1 foci is maintained in previously *Hp*-infected cells, whatever the genotoxic stress underwent by cells.

MKN45 cells were first infected with *Hp* 7.13 or not, as described in the supplementary information. After 24h, cells were washed 3 times and either treated or not with (A) MMS (1mM) and (B) H_2O_2 (1mM) for 24h as in figure 7A. IF analysis of USF1 (green) and p53 (red). Nuclei (Hoechst, blue) and phalloidin actin staining (grey). In both cases, either MMS or H_2O_2 post-infection treatment, USF1 foci are observed in the peripheral/cytoplasmic parts of cells, as observed in CPT-treated cells 24h post-*Hp* infection (see figure 7B). Scale bar 5µm.

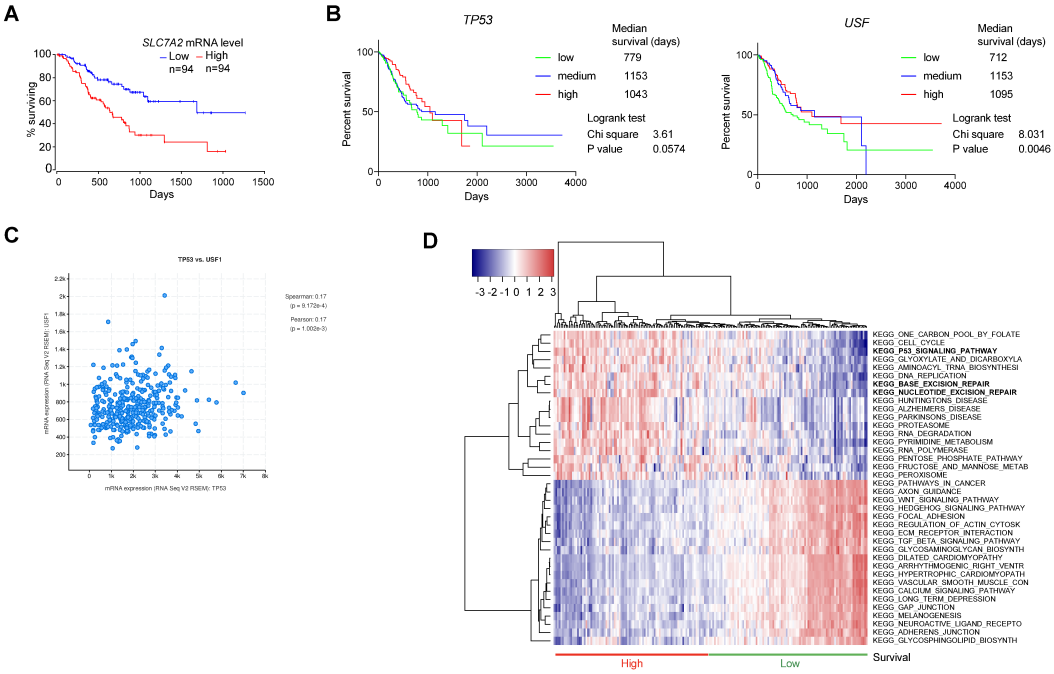
A
SLC7A2 mRNA level
Low n=94
High n=94
% surviving
Days
B
TP53
Median survival (days)
low 779
medium 1153
high 1043
Logrank test
Chi square 3.61
P value 0.0574
Percent survival
Days
USF
Median survival (days)
low 712
medium 1153
high 1095
Logrank test
Chi square 8.031
P value 0.0046
Percent survival
Days
C
TP53 vs. USF1
D
-3 -2 -1 0 1 2 3
KEGG_ONE_CARBON_POOL_BY_FOLATE
KEGG_CELL_CYCLE
KEGG_P53_SIGNALING_PATHWAY
KEGG_GLYOXYLATE_AND_DICARBOXYLA
KEGG_AMINOACYL_TRNA_BIOSYNTHESI
KEGG_DNA_REPLICATION
KEGG_BASE_EXCISION_REPAIR
KEGG_NUCLEOTIDE_EXCISION_REPAIR
KEGG_HUNTINGTONS_DISEASE
KEGG_ALZHEIMERS_DISEASE
KEGG_PARKINSONS_DISEASE
KEGG_PROTEASOME
KEGG_RNA_DEGRADATION
KEGG_PYRIMIDINE_METABOLISM
KEGG_RNA_POLYMERASE
KEGG_PENTOSE_PHOSPHATE_PATHWAY
KEGG_FRUCTOSE_AND_MANNOSE_METAB
KEGG_PEROXISOME
KEGG_PATHWAYS_IN_CANCER
KEGG_AXON_GUIDANCE
KEGG_WNT_SIGNALING_PATHWAY
KEGG_HEDGEHOG_SIGNALING_PATHWAY
KEGG_FOCAL_ADHESION
KEGG_REGULATION_OF_ACTIN_CYTOSK
KEGG_ECM_RECEPTOR_INTERACTION
KEGG_TGF_BETA_SIGNALING_PATHWAY
KEGG_GLYCOSAMINOGLYCAN_BIOSYNTH
KEGG_DILATED_CARDIOMYOPATHY
KEGG_ARRHYTHMOGENIC_RIGHT_VENTR
KEGG_HYPERTROPHIC_CARDIOMYOPATH
KEGG_VASCULAR_SMOOTH_MUSCLE_CON
KEGG_CALCIUM_SIGNALING_PATHWAY
KEGG_LONG_TERM_DEPRESSION
KEGG_GAP_JUNCTION
KEGG_MELANOGENESIS
KEGG_NEUROACTIVE_LIGAND_RECEPTO
KEGG_ADHERENS_JUNCTION
KEGG_GLYCOSPHINGOLIPID_BIOSYNTH
High
Low
Survival
E
Genes directly bound and regulated by TP53 (GSEA)
Enrichment plot: Fischer_direct_p53.grp
Top 25 p53 regulated genes enriched in high survival population
Top 25 p53 regulated genes enriched in low survival population
n=292
F
Genes having at least one occurence of the transcription factor binding site V$USF_01 (v7.4 TRANSFAC) in the regions spanning up to 4 kb around their transcription starting sites.
Enrichment plot: USF.grp
Top 25 USF1 regulated genes enriched in high survival population
Top 25 USF1 regulated genes enriched in low survival population
n=241
G
p=0.059
Fold change Tumor/healthy tissues
Hp-negative
Hp-positive

Figure S1

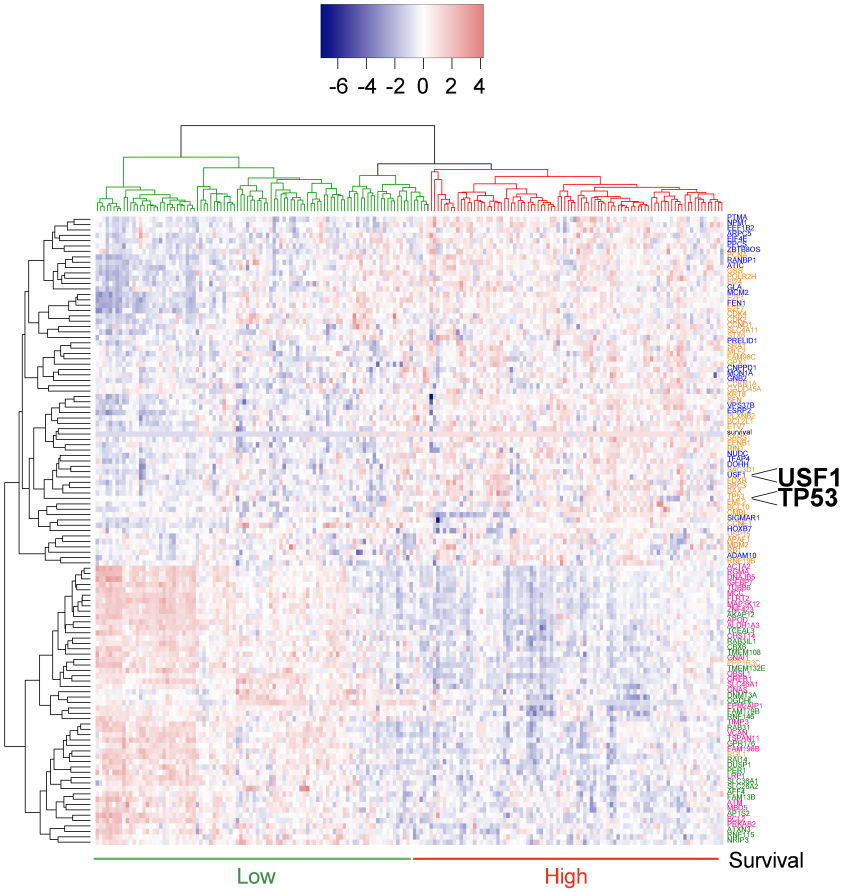

Figure S2

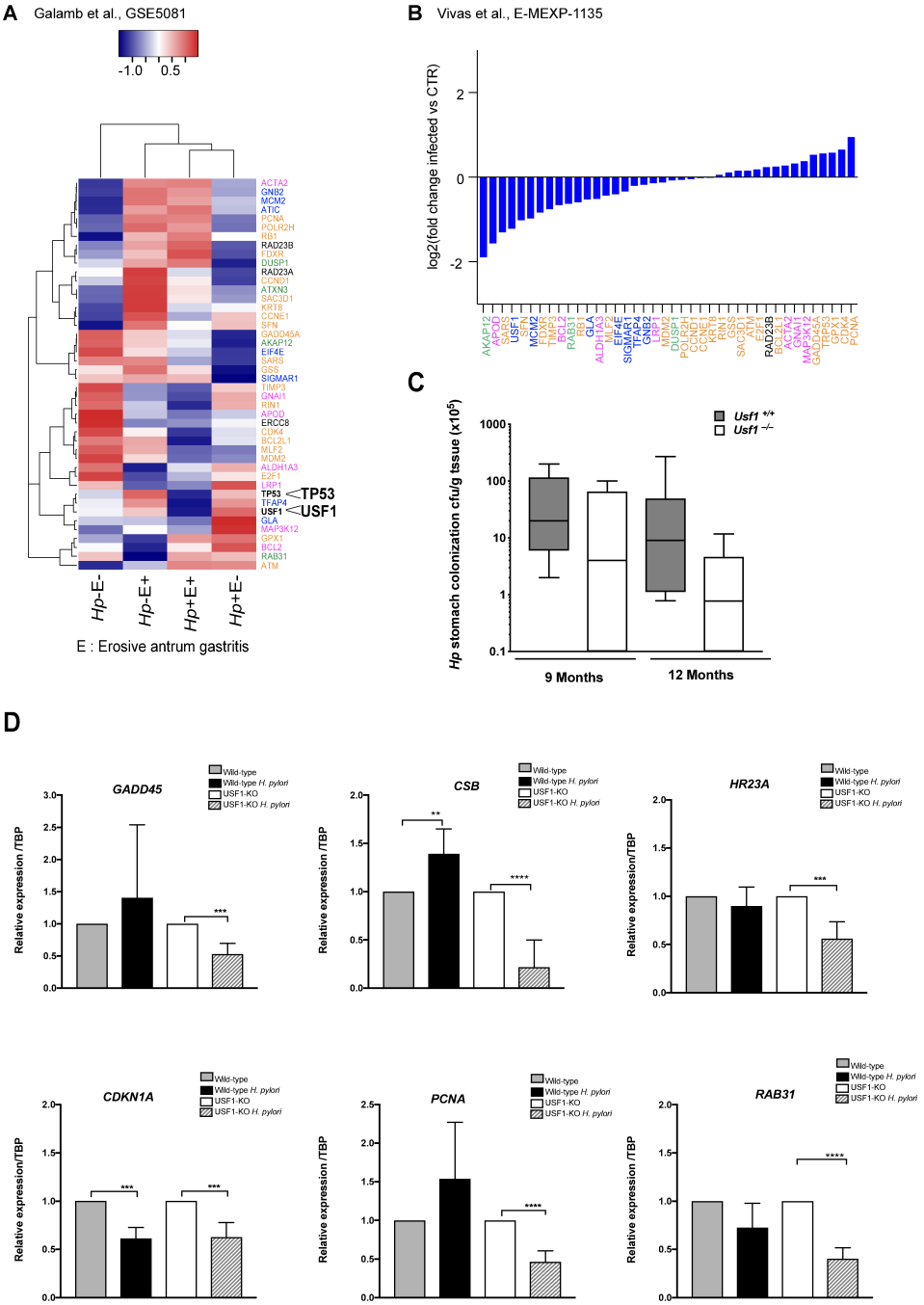
A
Galamb et al., GSE5081
-1.0 0.5
ACTA2
GNB2
MCM2
ATIC
PCNA
POLR2H
RB1
RAD23B
FDXR
DUSP1
RAD23A
CCND1
ATXN3
SACS1D1
KRT8
CCNE1
SFN
GADD45A
AKAP12
EIF4E
SARS
GSS
SIGMAR1
TIMP3
GNA11
RIN1
APOD
ERCC8
CDK4
BCL2L1
MLF2
MDM2
ALDH1A3
E2F1
LRP1
TP53
TFAP4
USF1
GLA
MAP3K12
GPX1
BCL2
RAB31
ATM
TP53
USF1
Hp-E-
Hp-E+
Hp+E+
Hp+E-
E : Erosive antrum gastritis
B
Vivas et al., E-MEXP-1135
log2(fold change infected vs CTR)
2
0
-2
AKAP12
APOD
SARS
USF1
SFN
MCM2
TIMP3
TFAP4
BCL2L1
RAB31
GLA
ALDH1A3
MLF2
EIF4E
SIGMAR1
TRAP2
GSS
LRP1
MDM2
DUSP1
RB1
POLR2H
CCND1
CCNE1
KRT8
RIN1
GPX1
SACS1D1
ATM
FDXR
RAD23B
BCL2L1
ACTA2
GNA11
MAP3K12
GADD45A
TP53
GPX1
CDK4
PCNA
C
Usf1 +/+
Usf1 −/−
Hp stomach colonization cfu/g tssue (x10^5)
1000
100
10
1
0.1
9 Months
12 Months
D
GADD45
CSB
HR23A
CDKN1A
PCNA
RAB31
Wild-type
Wild-type H. pylori
USF1-KO
USF1-KO H. pylori
Relative expression /TBP
Relative expression/TBP

Figure S3

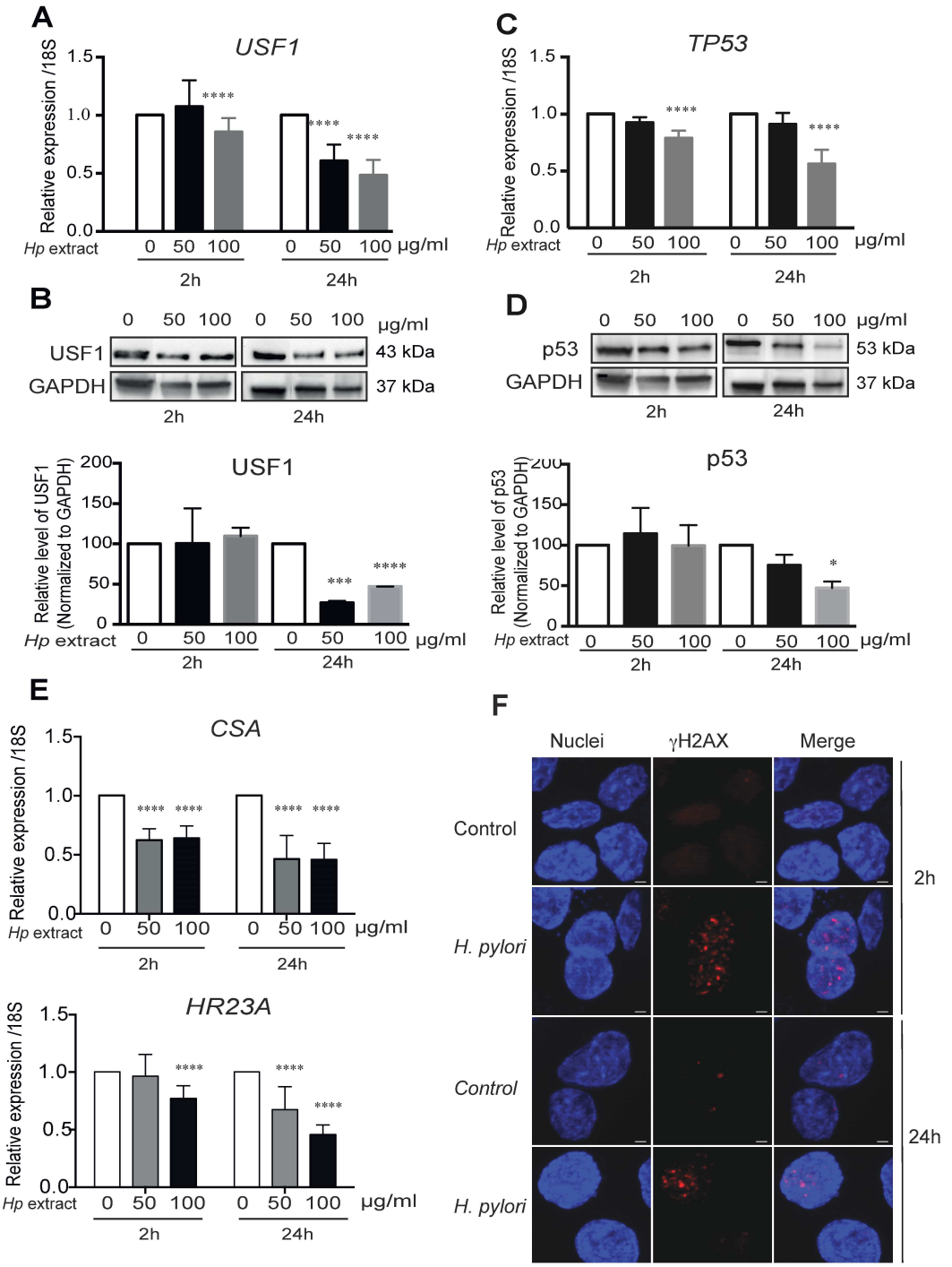
A
USF1
Relative expression /18S
1.5
1.0
0.5
0.0
****
****
****
Hp extract
0 50 100 0 50 100 µg/ml
2h
24h
B
0 50 100 0 50 100 µg/ml
USF1
43 kDa
GAPDH
37 kDa
2h
24h
C
TP53
Relative expression /18S
1.5
1.0
0.5
0.0
****
****
Hp extract
0 50 100 0 50 100 µg/ml
2h
24h
D
0 50 100 0 50 100 µg/ml
p53
53 kDa
GAPDH
37 kDa
2h
24h
USF1
Relative level of USF1 (Normalized to GAPDH)
200
150
100
50
0
***
****
Hp extract
0 50 100 0 50 100 µg/ml
2h
24h
p53
Relative level of p53 (Normalized to GAPDH)
200
150
100
50
0
*
Hp extract
0 50 100 0 50 100 µg/ml
2h
24h
E
CSA
Relative expression /18S
1.5
1.0
0.5
0.0
****
****
****
****
Hp extract
0 50 100 0 50 100 µg/ml
2h
24h
HR23A
Relative expression /18S
1.5
1.0
0.5
0.0
****
****
****
Hp extract
0 50 100 0 50 100 µg/ml
2h
24h
F
Nuclei
γH2AX
Merge
Control
H. pylori
Control
H. pylori
2h
24h

Figure S4

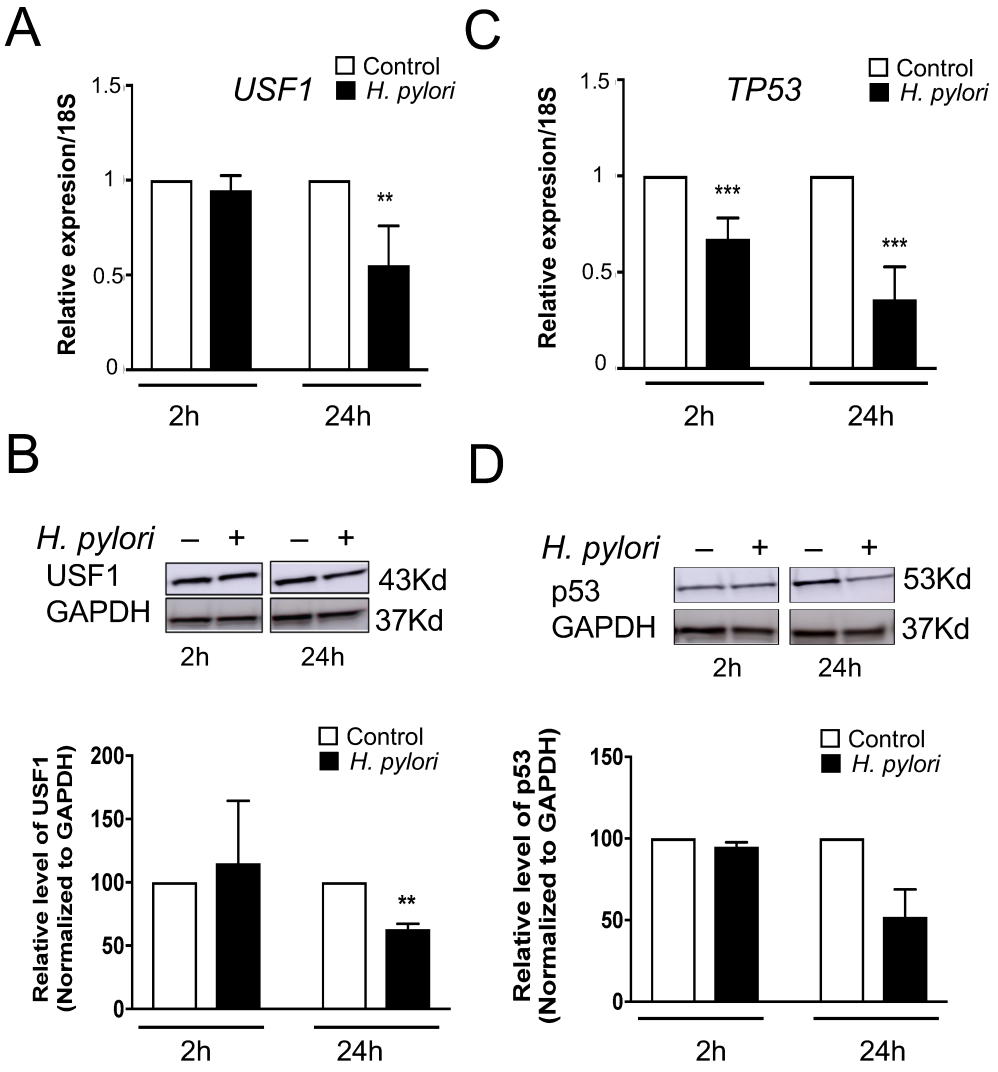
A
USF1
Control
H. pylori
Relative expresion/18S
1.5
1
0.5
0
**
2h
24h
C
TP53
Control
H. pylori
Relative expresion/18S
1.5
1
0.5
0
***
***
2h
24h
B
H. pylori – + – +
USF1
GAPDH
43Kd
37Kd
2h
24h
Control
H. pylori
Relative level of USF1 (Normalized to GAPDH)
200
150
100
50
0
**
2h
24h
D
H. pylori – + – +
p53
GAPDH
53Kd
37Kd
2h
24h
Control
H. pylori
Relative level of p53 (Normalized to GAPDH)
150
100
50
0
2h
24h

Figure S5

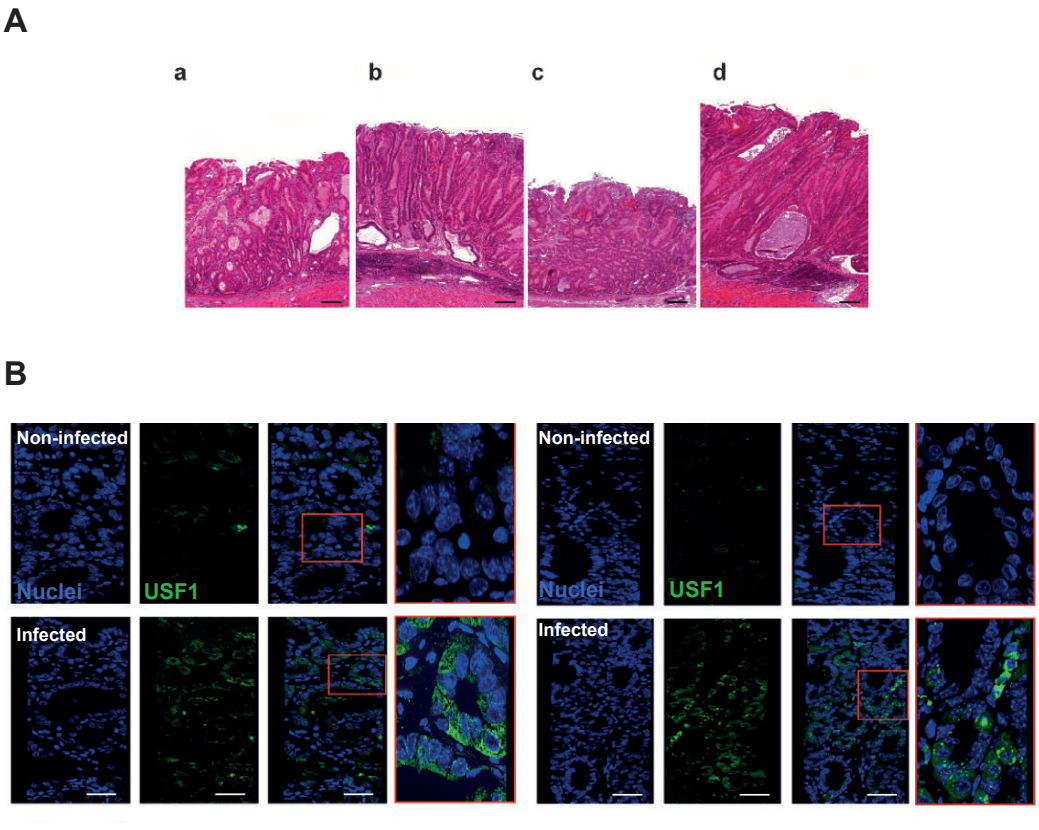
A
a
b
c
d
B
Non-infected
Nuclei
USF1
Infected
C
Non-infected
Nuclei
p53
Infected

Figure S6

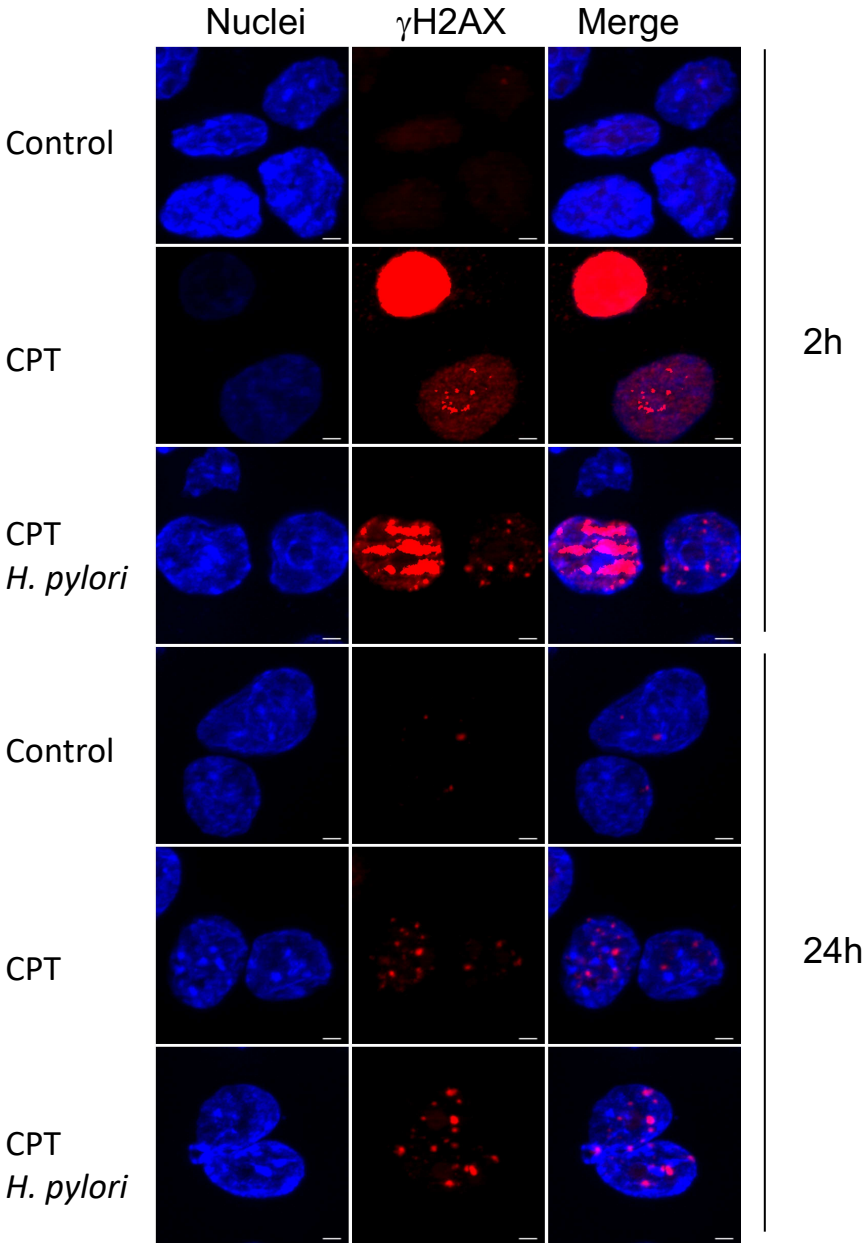
Nuclei
γH2AX
Merge
Control
CPT
CPT
H. pylori
2h
Control
CPT
CPT
H. pylori
24h

Figure S7

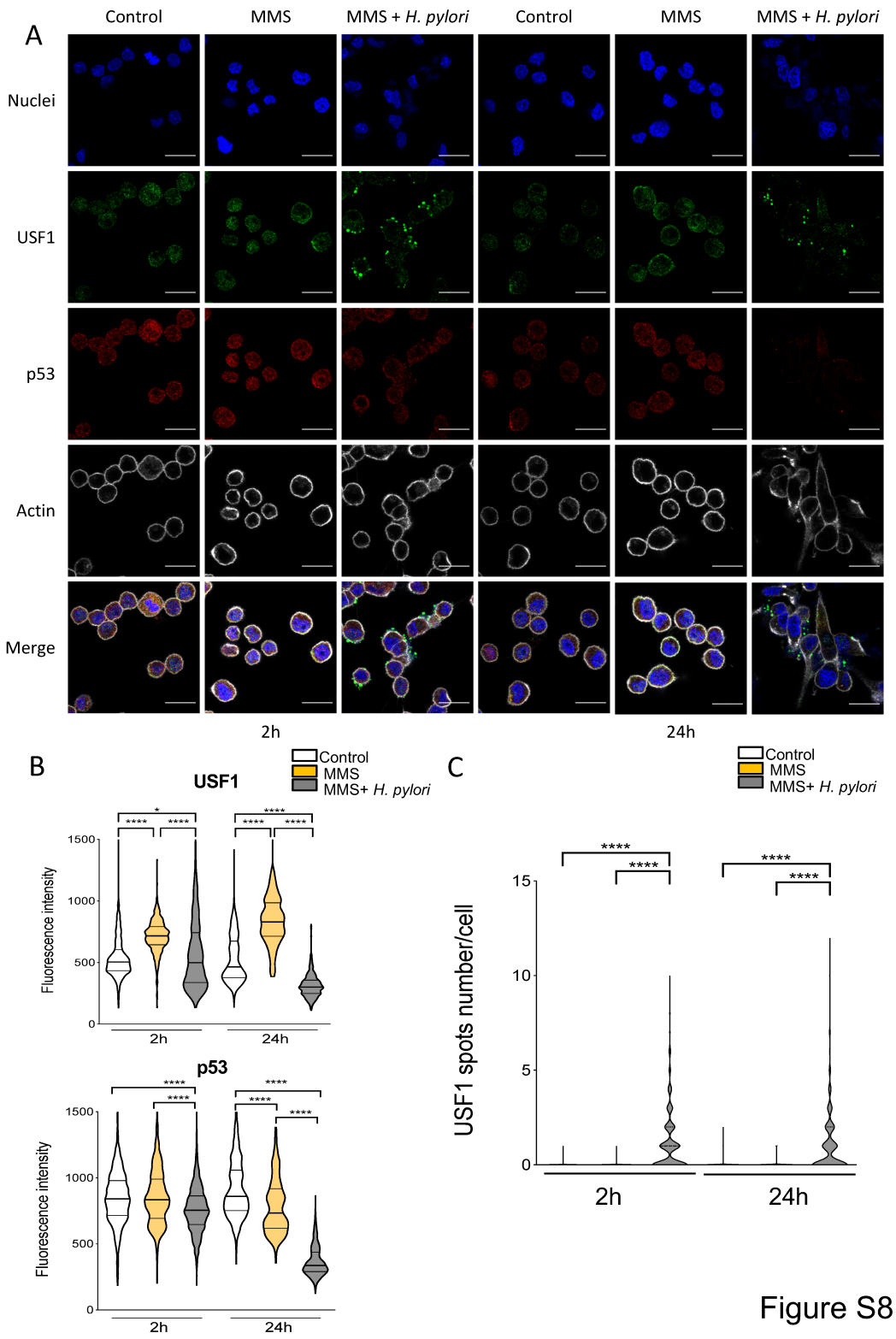
A
Control
MMS
MMS + H. pylori
Control
MMS
MMS + H. pylori
Nuclei
USF1
p53
Actin
Merge
2h
24h
B
USF1
Control
MMS
MMS+ H. pylori
Fluorescence intensity
1500
1000
500
0
2h
24h
p53
C
USF1 spots number/cell
15
10
5
0
****

Figure S8

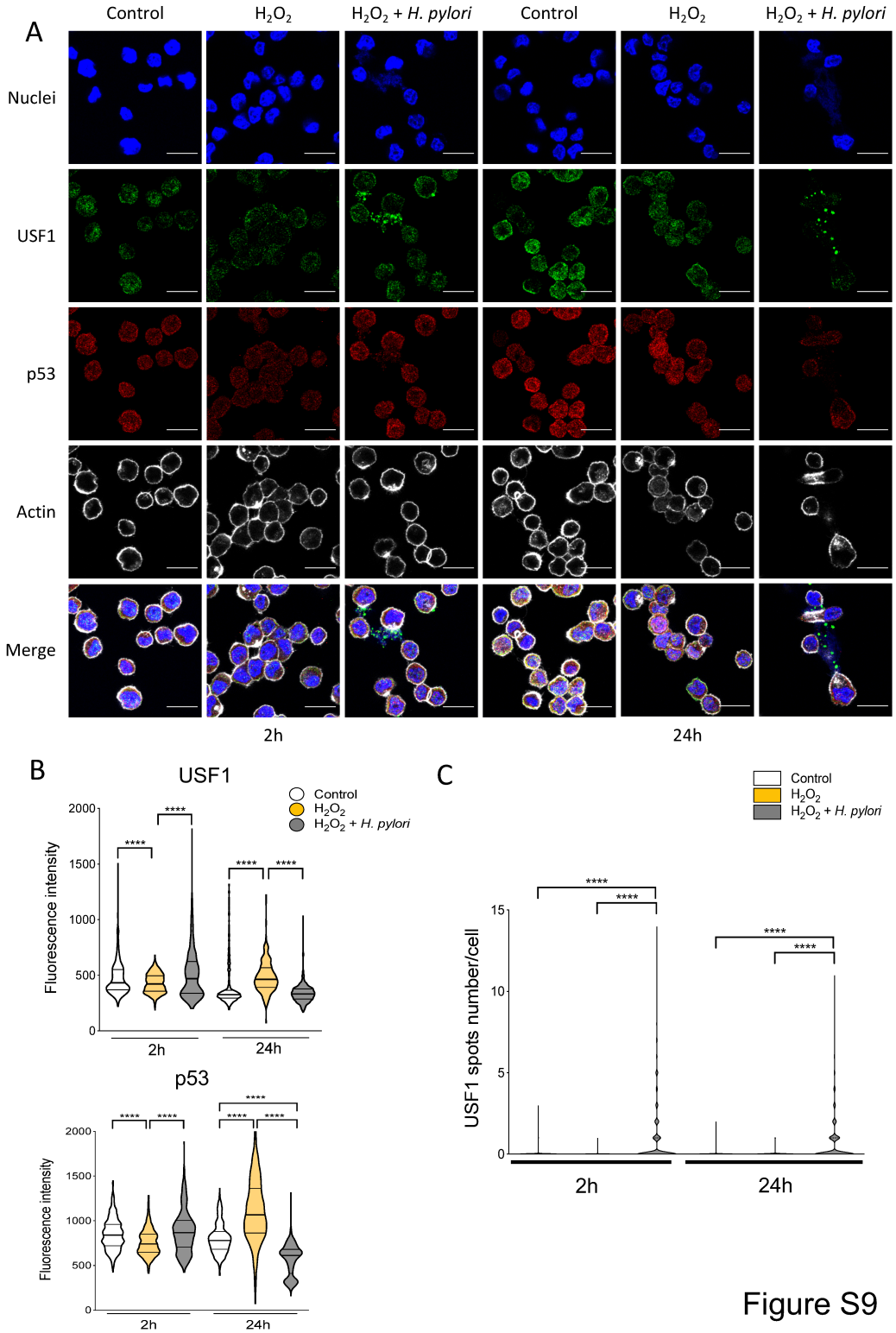
A
Control
H2O2
H2O2 + H. pylori
Control
H2O2
H2O2 + H. pylori
Nuclei
USF1
p53
Actin
Merge
2h
24h
B
USF1
Control
H2O2
H2O2 + H. pylori
Fluorescence intensity
2000
1500
1000
500
0
****
2h
24h
p53
Fluorescence intensity
C
Control
H2O2
H2O2 + H. pylori
USF1 spots number/cell
15
10
5
0
****
2h
24h

Figure S9

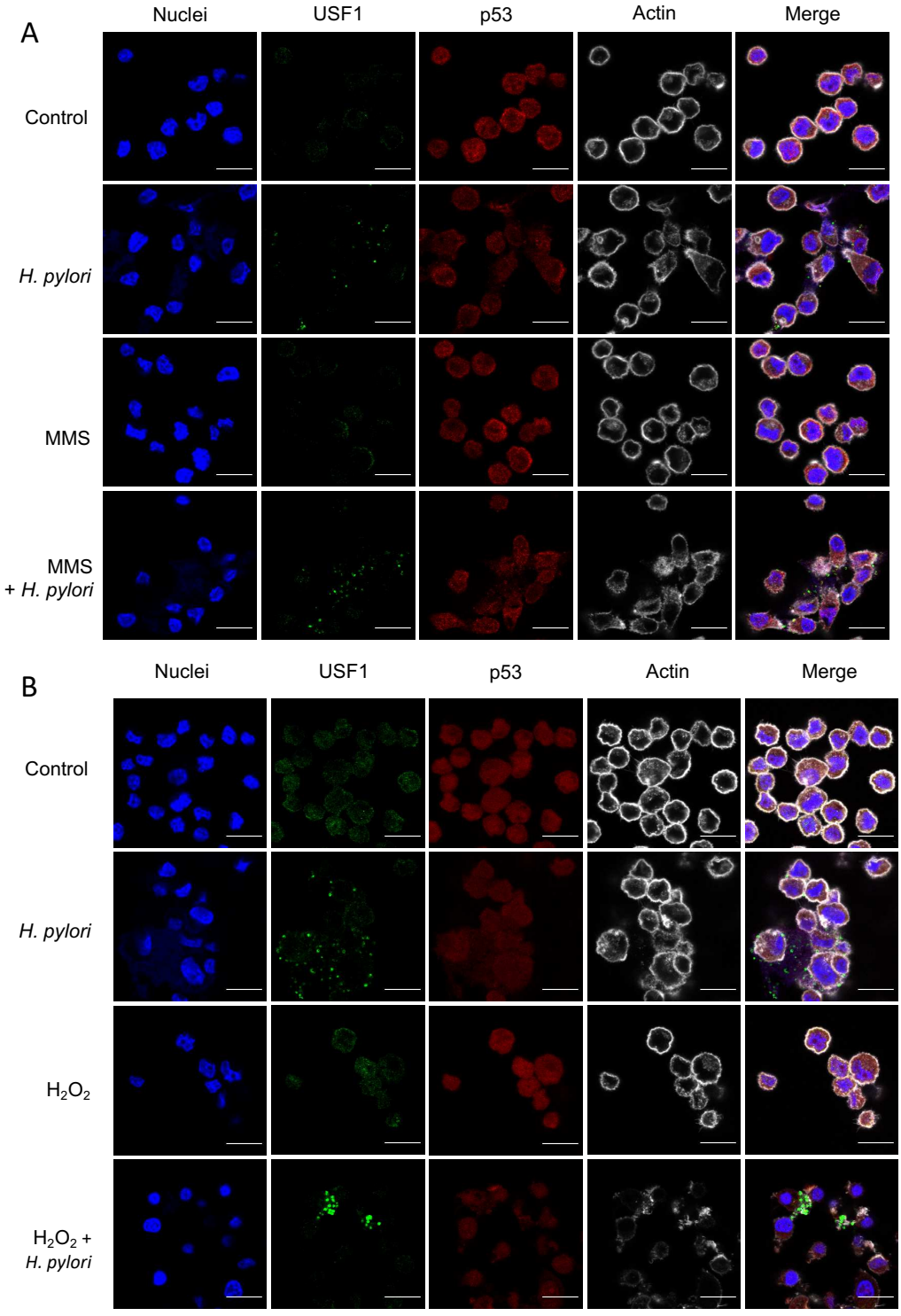
A
Nuclei
USF1
p53
Actin
Merge
Control
H. pylori
MMS
MMS
+ H. pylori
B
Nuclei
USF1
p53
Actin
Merge
Control
H. pylori
H2O2
H2O2 +
H. pylori

Figure S10